**The 1st International Conference on Local Resource Exploitation**
www.lorexp.org / info@lorexp.org
***REF: LOREXP_2021_A1212 Pages: 234–244***

LOREXP
LOCAL RESOURCE EXPLOITATION

# Prospective study on the parametric estimation of the spatial diffusion of a phenomenon: case study of cocoa black pod rot disease

## *Etude prospective sur l'estimation paramétrique de la diffusion spatiale d'un phénomène : étude de cas de la maladie de la pourriture noire des cabosses du cacao*

David Jaurès Fotsa-Mbogne[1,3,4,*], Jean Pierre Nken-Tchalle[2,4], Laurent Bitjoka[2,4]

[1] Department of Mathematics and Computer Science, ENSAI, The university of Ngaoundere
[2] Department of Electrical, Automatic and Energetic Engineering, ENSAI, The university of Ngaoundere
[3] Laboratory of Mathematics, Computer Science and Applications, FS, The University of Ngaoundere,
[4] Laboratory of Electrical, Signal, Image and Automatic, ENSAI, The university of Ngaoundere
* Corresponding Author: jauresfotsa@gmail.com

## ABSTRACT:

Progression evaluation is a necessity for optimal control of a phytopathology such as cocoa brown rot. One of the main questions is when to proceed with sanitary harvesting of infected pods. Unfortunately, non-destructive monitoring approaches (by imaging) are either very expensive or limited to area estimation. Thus, our objective is to develop a non-destructive method of volume estimation. To achieve our goal, we build a 3D mathematical model of disease progression based on Markovian process with jumps inspired by the literature. We also build a parametric estimator using the maximum likelihood method, which allows us to apply the known methods of disease progression evaluation. The particularity of our model is that it takes into account the particular geometry of the cocoa pods whose surface is put in bijection with the 2D image which acts as input of the proposed estimator. The convergence of the proposed estimator towards the characteristic parameter sought is exponential according to a significant statistical model whose expression is given ($R^2 = 71.34\,\%$ and $p - value = 2.68 \times 10^{-9}$). The estimation error of the severity of the disease converges by upper value to 0; this is better than an underestimation with regard to the control decisions to be taken.

**Keywords**: Plant disease, monitoring, maximum likelihood estimator, non-destructive methods.

## RÉSUMÉ :

L'évaluation de la progression est une nécessité pour un contrôle optimal d'une phytopathologie telle que la pourriture brune du cacao. L'une des principales questions est de savoir quand procéder à la récolte sanitaire des cabosses infectées. Malheureusement, les approches de suivi non destructif´ (par imagerie) sont soit très couteuses, soit limitées à l'estimation de la surface. Ainsi, notre objectif` est de développer une méthode non-destructive d'estimation du volume. Pour atteindre notre objectif, nous construisons un modèle mathématique 3D de la progression de la maladie basé sur un processus´ markovien avec sauts inspire de la littérature. Nous construisons également un estimateur paramétrique utilisant la méthode du maximum de vraisemblance, ce qui nous permet d'appliquer les méthodes connues d'évaluation de la progression de la maladie. La particularité de notre modèle est qu'il prend en` compte la géométrie particulière de la cabosse de cacao dont la surface est mise en bijection avec l'image 2D qui sert d'entrée à l'estimateur proposé. La convergence de l'estimateur proposé vers le paramètre caractéristique recherchée est exponentielle selon un modèle statistique significatif dont l'expression est donnée ($R^2 = 71{,}34\,\%$ and $p - value = 2{,}68 \times 10^{-9}$). L'erreur d'estimation de la gravite de la maladie converge par valeur supérieure vers 0 ; ce qui est mieux qu'une sous-estimation au regard des décisions de lutte prendre.

**Mots clés** : Phytopathologie, diffusion spatiale, surveillance, estimateur du maximum de vraisemblance, méthode non destructive.

## 1. INTRODUCTION

Seventy five percent of the world's poor live in a rural zone with agricultural activities as their major source of livelihood (Da Silva et al., 2009). Agro-industries stand as one of the solutions for reducing poverty in the world (Da Silva et al., 2009; Takoyoh, 2003 and Townsend et al., 2013). The agro-industries can be defined as sectors based on all activities of transformation, packaging, distribution and production of agricultural products such as cocoa. The cocoa tree belongs to a group of small trees found in the wild in the Amazon basin and other tropical regions of South and Central America. There are more than twenty species of cocoa tree but the *Theobroma cacao L.* is the only one to be cultivated on a large scale (Wood et Lass, 2008). It is divided into three groups: Criollo, Trinitario and Forastero. The Farastero group accounts for almost 80 % of world production. The fruit of the cocoa tree is a berry, called cherelle at the beginning of its development, then pod. A pod has an estimated size of about 20$cm$ and can weigh 400 $g$ containing 100 $g$ of fresh beans. The pod contains about forty more or less plump, almond-shaped beans surrounded by a sweet and sour mucilaginous pulp (citric acid) fixed on a central rachis. Beans are rich in fats, polyphenols, proteins and alkaloids with stimulating properties (theobromine and caffeine) (Barel, 1985 and Magrone, 2017). The cocoa tree was established in Cameroon at the end of the 19th century. According to the World Trade Organization, cocoa activity in Cameroon contributes to 3 % of Gross Domestic Product (GDP) and 6 % of primary GDP supporting about 600,000 producers whose income was estimated at more than 250 billion CFA francs in 2010 (Kanmogne et al., 2012). A detailed study of the organization of the cocoa sector in Cameroon is presented in (Bagal et al., 2013). Unfortunately, between 20-40 % of the annual cocoa crop yield is lost due to pests and diseases (Ling et al., 2019; Perrine-Walker, 2020 and Bismark et al., 2020). The most important disease is cocoa black pod rot, which is due to several species of *Phytophthora* (Perrine-Walker, 2020 and Nembot et al., 2018). The black pod disease has an impact on cocoa beans (the constituents of the pod) and particularly to chocolate (Bismark et al., 2020).

According to Nembot et al. (2018) and references therein, cocoa black pod rot disease is generally controlled through fungicide applications, selection of partially resistant or tolerant cocoa cultivars and cultural practices (phytosanitation). Phytosanitary pod removal consists of cleaning trees at the beginning of the season by removing mummified fruits left from the previous season, and the subsequent regular removal of diseased pods, which are the source of secondary inoculum. Phytosanitation is time consuming and relatively difficult to put in place. Fungicide applications are effective yet, but have numerous negative externalities, such as human health problems, pollution, reductions in the populations of beneficial organisms, and emergence of secondary diseases or pathogen resistance to pesticides. An appropriate combination of these control methods can increase the effectiveness (Nembot et al., 2018; Fotsa-Mbogne and Thron, 2015 and Ndoungue et al., 2018). The optimal control strategy being generally given such as a feedback of state variables, their evaluation based on an accurate model considering stochastic nature of phenomena of interest is recommended (Fotsa-Mbogne, 2018). There are several attempts to model the spatio-temporal dynamics of diseases, especially at the scale of the farm (Nembot et al., 2018; Marcelo and Edson, 2010; Gardner, 1970; Ndoumbe et al., 2017). However, it seems necessary to develop additional models at lower scales in order to better understand scale interactions and to adopt appropriate control strategies (Kleczkowski et al., 1997). For example, it might be not necessary to totally destruct a tree or to proceed to sanitary harvesting if a certain level of disease severity is not reached, and the optimal control measures might not be spatially uniform (Sebastian et al., 2021).

Such a precision can be difficult with traditional human approaches, but is easier with advanced technological tools such as image processing.

Imaging belongs to the class of non-destructive methods that includes spectroscopy, computer vision, thermography, hyperspectral imaging, magnetic resonance imaging, X-ray imaging, acoustic imaging, and chromatography. There are works on disease recognition and severity evaluation of plants using image-processing methods (Corkidi et al., 2006; Gittaly et al., 2018; Nader et al., 2016; Diego and Rafael, 2018 and Rady et al., 2017). Most work in the field is limited to analysis of the leaf or fruit surface (Corkidi et al., 2006; Gittaly et al., 2018and Diego and Rafael, 2018). Although there are efficient 3D imaging methods to monitor disease progression, they are expensive and difficult to apply in the farm (Nader et al., 2016; Rady et al., 2017; Abid Hussain et al., 2018; Anuja and Atul, 2018). Thus, it would be interesting to be able to estimate the 3D state of evolution of the disease just based on 2D surface images. Assuming that the 2D image processing is well done, the issue tackled in this work is that of to combine the sequence of disease states at the external surface of cocoa pod (observation) to a 3D mathematical model, in order to estimate 3D real dynamics of the disease (signal). Recently, Vermolen and Polonen (2020) proposed and proved the accuracy of a cancer diffusion model based on Poisson process theory applied to cellular automatons. The intensity of the process was not constant but proportional to a key constant λ. Given λ, it was possible to infer on the severity of the disease given its running period. It was also able to infer on the time the disease would invade a given proportion of a set of cells (50% for example).

By adopting the model developed by Vermolen and Polonen (2020), our objective is reduced to give a procedure allowing to estimate with precision the parameter λ. This will necessarily involve the study of the relationship between the estimate and the real value of λ, taking into account the geometry of the pod. Moreover, we intend to study the asymptotic behavior of the estimator in terms of absolute relative error. Hence, the remaining part of the paper has the following structure. In section 2, we present the methodology we use to model a cocoa pod (Subsection 2.1), to model the disease diffusion phenomenon (Subsection 2.2), and to estimate key control parameters. Section 3 is devoted to numerical simulations and discussions about the asymptotic behavior of proposed estimators of λ. We end by a conclusion in Section 4.

## 2. MODELING AND ESTIMATION METHODS

### 2.1. Geometrical modeling of cocoa black pod

Since the progression of the cocoa black pod disease is done step by step by cells, it is important to take into account the geometry of the pod. The cocoa pod can be easily modeled using cylindrical coordinates. It presents a 3D appearance of the revolution around the z-axis of a parabolic curve like a rugby ball. However, it has more or less regular longitudinal grooves that give it a rosette shape when viewed from above. Thus, we propose the following set $\wp$ to represent a cocoa pod:

$$\wp = \{(r, \theta, z) \in \mathbb{R}_+ \times ]-\pi, \pi] \times [0, H]; r \leq az(H - z)(b + \sin(c(\theta + \pi)))\}. \quad (1)$$

where $a, b, c, H > 0$. $H$ is the height of the cocoa pod and $\frac{a(b+1)H^2}{2}$ is its the maximal radius. The relation between a 2D image of cocoa pod surface and the real lateral surface is given by the following homeomorphism

$$\phi : I = [0,`] \times [0,L] \to \wp$$

$$(x,y) \mapsto \varphi(x,y) = \left(\frac{ayH^2}{L^2}\left(b + \sin\left(c\left(\frac{2\Pi x}{l}\right)\right)\right), \frac{\Pi(2x-l)}{l}, \frac{yH}{L}\right). \quad (2)$$

The function $\varphi$ can be extended on $R^2$as a periodical function: $\varphi(x,y) = \varphi(x\ mod\ l, y\ mod\ L)$. The parametric representation of a cocoa pod is graphically given in Figure 1.

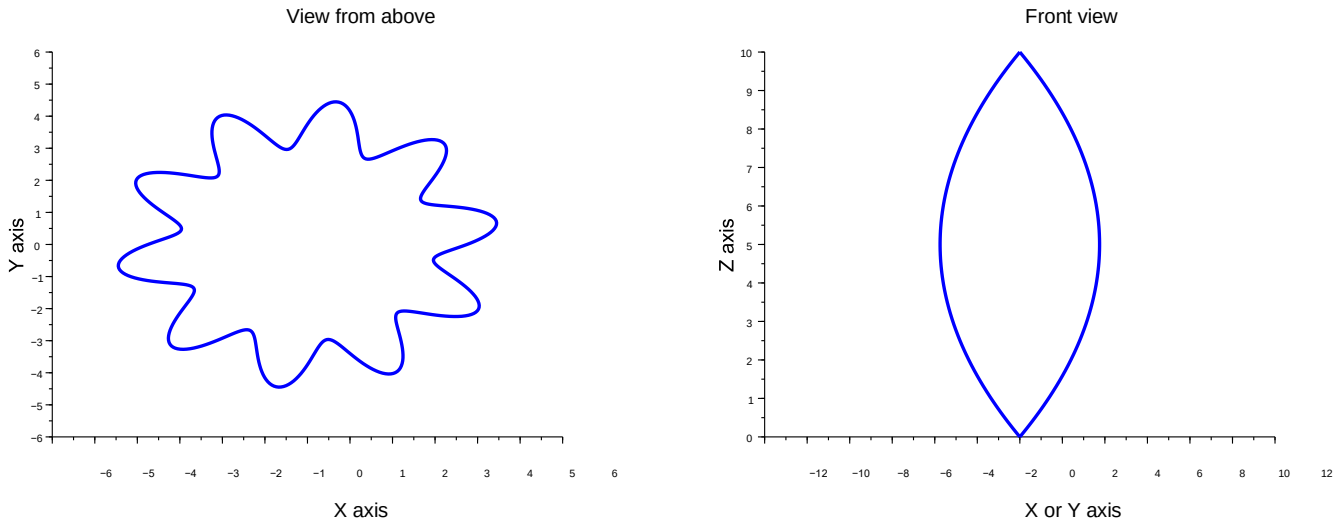


**Figure 1:** Parametric representation of cocoa pod

### 2.2. Modeling the diffusion cocoa black pod disease

Following the recent work of Vermolen and Polonen (2020), cancer diffusion is modeled using Poisson processes. Indeed, the time for a given susceptible cell *i* to become infected is assumed to follow an exponential law with a non constant intensity $\lambda_i$. $\lambda_i$ is a nonnegative function which depend upon the time ($t$) and the current distribution of infected cells. It is shown in Proposition 2.3 of Vermolen and Polonen (2020) that

$$\lambda_i(t) = \lambda \sum_{j \in \mathcal{N}_i \setminus \{i\}} \frac{S_j(t)}{d(x_i, x_j)}, \quad (3)$$

$\lambda$ being a positive constant, $\mathcal{N}_i$ being the nearest neighborhood of cell $i$ in the cocoa pod, $S_j(t) \in \{0,1\}$ being the state of the cell $j$ at time $t$ ($S_j = 1$ if the cell is infected and $S_j = 0$ otherwise), $x_j$ being the spatial position cell $j$ and $d(x_i, x_j)$ being the distance between positions $x_i$ and $x_j$. We adopt a similar approach in this work.

Let $p(t_0, t_0 + dt, i)$ denote the probability that a susceptible cell $i$ becomes infected between the time $t_0$and the time $t_0 + dt$ . Then conditionally upon $S_i(t_0) = 0$, $S_i(t_0 + dt)$ follows a Bernoulli law $\mathfrak{B}(p(t_0, t_0 + dt, i))$, with

$$p(t_0, t_0 + dt, i) = \int_{t_0}^{t_0+dt} \lambda_i(s)\exp\left(-\int_{t_0}^{s} \lambda_i(\tau)d\tau\right)ds = 1 - \exp\left(-\int_{t_0}^{t_0+dt} \lambda_i(s)\, ds\right). \quad (4)$$

As a Poisson process, the number of infected cells is an increasing process which is piecewise constant. We will assume for a sake of simplicity that the difference between two times of observation of the disease evolution is a given constant $\Delta t$. We additionally suppose that $\lambda_G = \sum_{i=1}^{n_{cells}} \lambda_i(1 - S_i)$ is constant between two observations. Given a time $t_0$, the average time to spend before the next infection is

$$\Delta t(t_0) = \int_{t_0}^{+\infty} s\lambda_G(s)\exp\left(-\int_{t_0}^{s} \lambda_G(\tau)d\tau\right)ds - t_0 = \int_{t_0}^{+\infty} \exp\left(-\int_{t_0}^{t} \lambda_G(s)ds\right)dt. \quad (5)$$

Thus, the above hypothesis means that

$$p(t_0, t_0 + \Delta t, i) = 1 - \exp\big(-\lambda_i(t_0)\Delta t(t_0)\big). \quad (6)$$

### 2.3. Estimation of diffusion parameter $\lambda$

As we have seen before, the dynamics of the disease is strongly related to the value of the parameter $\lambda$. Thus, the objective of this section is to give a reliable procedure of estimation of $\lambda$. We use the maximum likelihood method by considering the maximization of the likelihood function

$$\mathcal{L}_n(x) = \prod_{k=1}^{n} \prod_{i \in \partial\wp} f(i, k, S_i(t_{k-1}),\ S_i(t_k)), \quad (7)$$

where

$$f\big(i, k, S_i(t_{k-1})\ S_i(t_k)\big) = \max\big\{S_i(t_{k-1}), 1 - S_i(t_k)\big(1 - \omega_{i,k}\lambda \exp\big(-\omega_{i,k}\lambda\Delta t\big)\big)\big\}, \quad (8)$$

where $\omega_{i,k} = \sum_{j \in \wp_k \cap \mathcal{N}_i\{i\}} \frac{S_j(t_{k-1})}{d(x_i,\ x_j)}$ and $\wp_k \subseteq \partial\wp$ is the subset of newly infected cells at the cocoa pod surface. $\mathcal{L}_n$ represents the probability of a given infection scenario from time 0 to time *n*. The Likelihood function $\mathcal{L}_n$ is not classical because it is a conjoint law of sequence of independent random variables not having the same law. However, the fact that the likelihood in not constructed based on a classical sampling does not affect the estimation procedure since the parameter $\lambda$ is constant. $\mathcal{L}_n$ can be rewritten as:

$$\mathcal{L}_n(x) = \prod_{k=1}^{n}\Big(\prod_{i \in \wp_k} \lambda\omega_{i,k}\Big) \exp\Big(-\Big(\sum_{i \in \wp_k} \omega_{i,k}\Big)\lambda\Delta t\Big). \quad (9)$$

If $N_n$ denotes the number of infected cells at the surface of a cocoa pod after $n$ steps of time, then the log-likelihood is given by

$$\ln\left(\mathcal{L}_n(x)\right) = N_n \ln\left(\lambda\right) + \sum_{k=1}^{n}\Big(\sum_{i \in \wp_k} \ln\left(\omega_{i,k}\right)\Big) - \Big(\sum_{k=1}^{n}\sum_{i \in \wp_k} \omega_{i,k}\Big)\lambda\Delta t \quad (10)$$

and the maximum likehood estimation of $\lambda$ is

$$\hat{\lambda}_1\left(\frac{1}{n}, \Delta t\right) = \frac{N_n}{\Big(\sum_{k=1}^{n}\sum_{i \in \wp_k} \omega_{i,k}\Big)\Delta t}. \quad (11)$$

By analogy with the biased nature of the maximum likelihood estimator for the exponential distribution (Lejeune, 2004), we also suggest the alternative estimation

$$\hat{\lambda}_2\left(\frac{1}{n}, \Delta t\right) = \frac{N_n - 1}{\Big(\sum_{k=1}^{n}\sum_{i \in \wp_k} \omega_{i,k}\Big)\Delta t}. \quad (12)$$

Notice that it sufficient to use $\Delta t = 1$ since $\lambda$ is a frequency and therefore includes the time unit.

Given an estimator $\hat{\lambda}$, it is very important to evaluate its bias and its quadratic mean error (Lejeune, 2004). In particular, we want to evaluate $\lim_{h \to 0} \mathbb{E}\big[\hat{\lambda}(\mathrm{h},\ 1)\big] - \lambda$ and $\lim_{h \to 0} \mathbb{E}\big[\hat{\lambda}^2(\mathrm{h},\ 1)\big]$. Using Proposition 6.11, page 127 of Lejeune (2004), the previous limits exist with $\lim_{h \to 0} \mathbb{E}\big[\hat{\lambda}^2(\mathrm{h},\ 1)\big] = 0$. Thus, we can only focus

on the asymptotic bias $\lim_{h\to 0} \mathbb{E}\left[\hat{\lambda}(h,\ 1)\right] - \lambda$. For a given $n \in N$ and $\Delta t \in \mathbb{R}_+^*$, we are able to estimate $\mathbb{E}\left[\hat{\lambda}(h,\ k)\right]$by sampling. Such a sampling is possible if several cocoa pods are followed in parallel.

## 3. RESULTS AND DISCUSSIONS

### 3.1. Simulation of disease diffusion

In this section, we present the simulation of disease diffusion according to the models we gave in Section 2.1 and Section 2.2. We used a computer having a processor Intel(R) Core (TM) i7-4600U CPU @2.10 GHz @2.70 GHz and 8Go of RAM.

Figure 2 presents a simulation of disease diffusion viewed at the surface of a cocoa pod (narrow cells). We can see some discontinuities meaning that the infection of a surface cell may come from the interior of the cocoa pod.

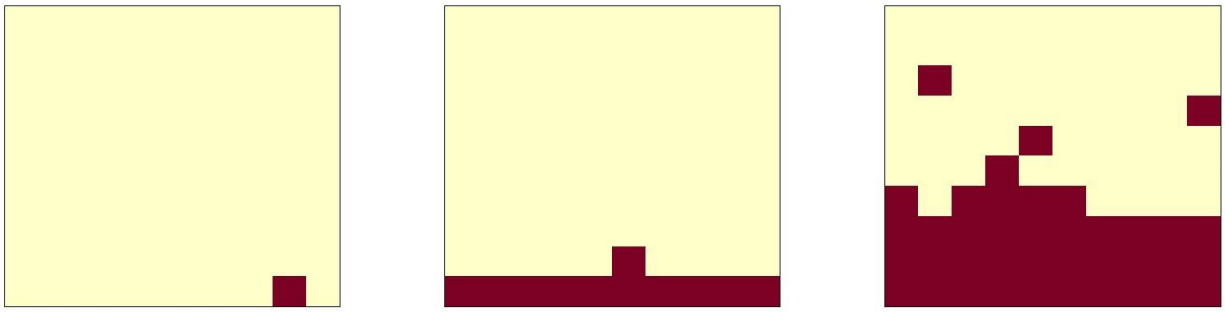

Step 1 Step 8 Step 16

**Figure 2:** Disease diffusion on cocoa pod surface with λ = 1

Figure 3 shows the simulation evolution of the prevalence of infected cells both at the surface and in the global cocoa pod. We observe that the 2D prevalence is higher than the 3D prevalence. Obviously, in terms of absolute values, the global number of infected cells is greater than the number of infected cells at the surface of cocoa pod.

### 3.2. Numerical Estimation of diffusion parameter $\lambda$

The aim of this section is to study the behavior of the estimator $\hat{\lambda}_i$ when $n$ tend to $+\infty$. We carried out several simulations for $h = 2^{-1},\ldots,31^{-1}$ and $\lambda = 1{,}1.2,\ldots,1.8$. We assume that the relation between $\hat{\lambda}_i$ and $\lambda$ is given such as

$$\lambda = a_{h,i}\hat{\lambda}_i(h,1) + b_{h,i}. \qquad (13)$$

Using linear regression, we estimate the $a_{h,i}$ 's and the $b_{h,i}$'s. Then we extrapolate $a_{0,i}$'s and the $b_{0,i}$'s. Figure 4 shows the evolution of the $a_{h,i}$ 's and the $b_{h,i}$'s with respect to $n = \frac{1}{n}$ for $\hat{\lambda}_1$and $\hat{\lambda}_2$. A stationarity seems to arise starting from $n = 21$.

Figure 5 shows the evolution of the absolute value of the relative error of estimation (AVREE) with respect to to $n = \frac{1}{n}$ for $\hat{\lambda}_1$and $\hat{\lambda}_2$ . AVREE has the advantage to be free of scale (ie independent of the value of $\lambda$) and therefore better validates the results. We can observe that AVREE is decreasing with respect to *n*. Performances of $\hat{\lambda}_1$and $\hat{\lambda}_2$ are quite similar but $\hat{\lambda}_2$ seems to have a better the least absolute error. A log-normal regression model (with $R^2 = 71.34\,\%$ and $p - \text{value} = 2.68 \times 10^{-9}$) permits to empirically predict the dynamics of the absolute relative error according to $\hat{\lambda}_2$:

$$AVREE2 = exp(-0.0607419n + 6256787). \quad (14)$$

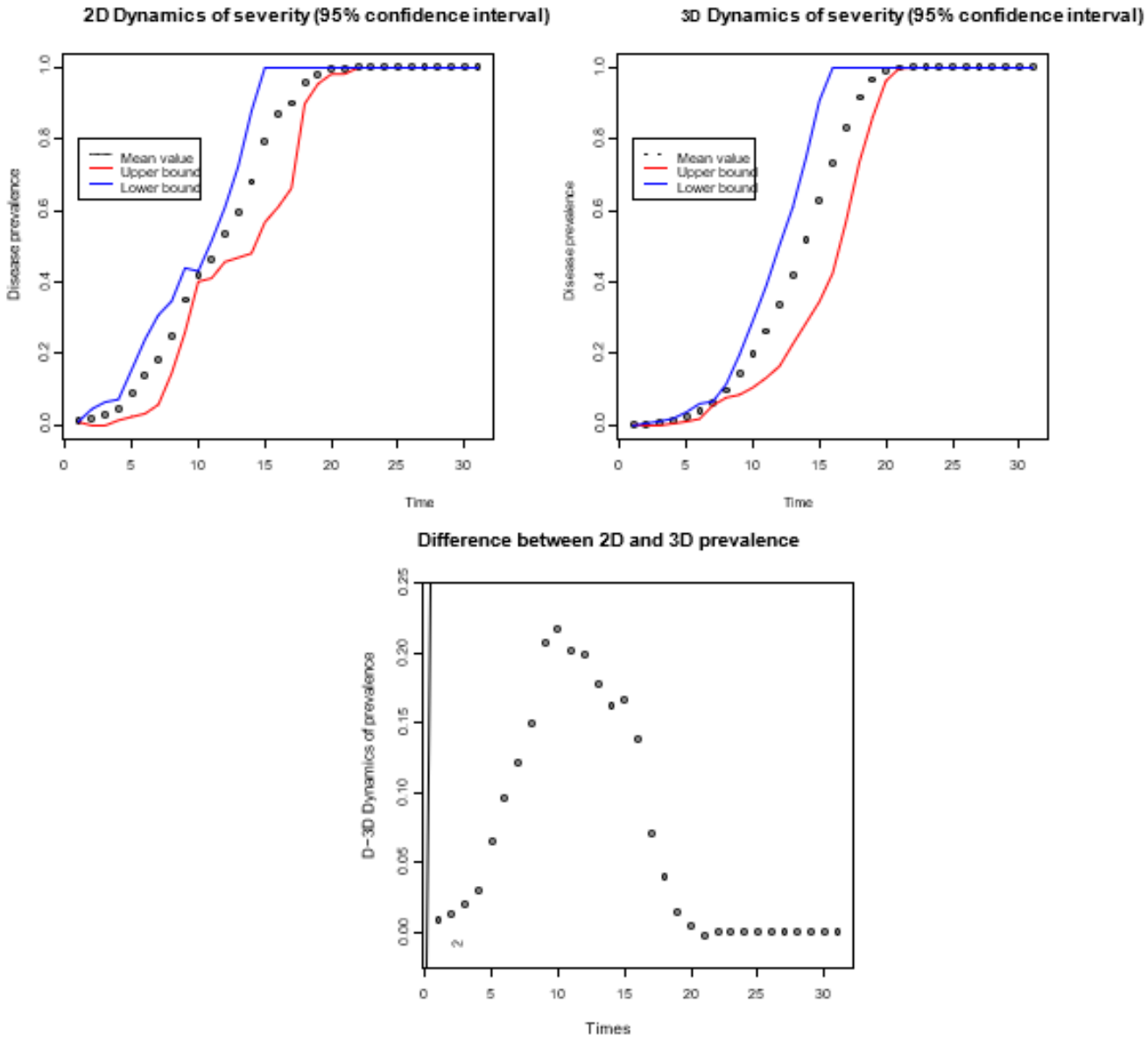


**Figure 3:** Disease prevalence dynamics with $\lambda = 1$

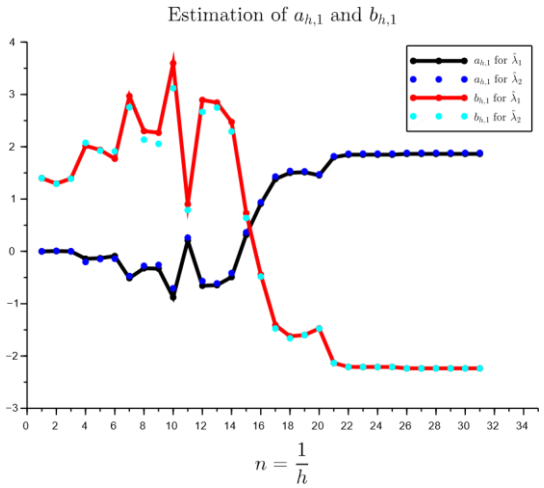


**Figure 4:** Estimation of $a_{1,i}$ and the $b_{1,i}$

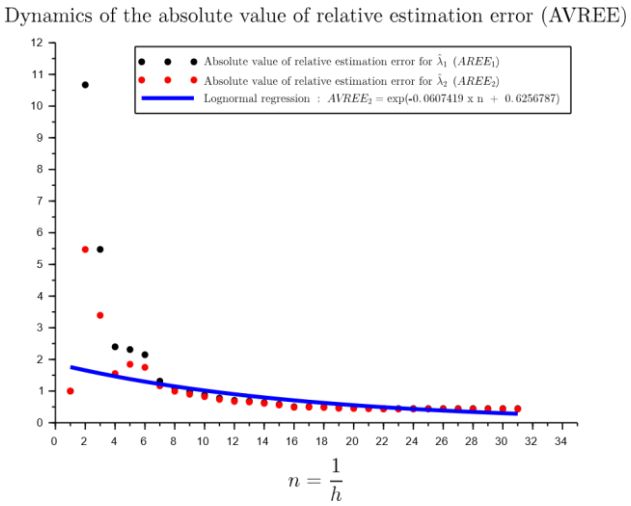


**Figure 5:** Evaluation of absolute relative error of estimation and empirical modeling

## 4. CONCLUSION

It was question in this work of the estimation of the progression of the brown rot of the cocoa pod. This estimation is necessary for a good decision making as for the control of the dynamics of the disease whose damage is prejudicial to the productivity and the quality of the product. Existing non-destructive estimation techniques being expensive or exclusively limited to surface scattering, we have proposed an original 3D estimation approach based on 2D image observations. Our approach has been to model the 3D diffusion of the disease by a parametric Markovian model with jumps. The model takes into account the geometry of the pod and allows to identify its surface with a 2D image whose evolution is used as input for the estimation procedure. The proposed model being mono-parametric, the estimation of its parameter is sufficient to apply known estimation methods such as Monte Carlo, which is widely used in the literature. Thus, we have constructed an estimator by the maximum likelihood method. Through a statistical study of regression, the latter converges exponentially to the estimated parameter according to a model whose adjustment rate is $R^2 = 71.34\,\%$ *and the* $p - value$ *is* $p - value = 2.68 \times 10^{-9}$. With regard to the results obtained, the non-destructive 3D estimation of the disease dynamics on the basis of surface observation is a fact thanks to an adequate combination of mathematical model and "simple" image analysis.

Although the relatively promising numerical behavior of the proposed estimator we expect to carry out further theoretical studies. Indeed, it is important to determine the probability law followed by an estimator in order to better evaluate among others the bias, the quadratic mean error and the confidence intervals. If it is established that the estimator is biased, we will be able to give an unbiased version of it. The current analysis assumed a constant step of time between two consecutive observations but it could be practically difficult to implement it. Hence, it would be interesting to adapt the estimator to that situation. Moreover, we focused on an exponential distribution that can be generalized by Weibull's, Gamma and Gompertz distributions, which have richer properties. A combination with kriging methods could be also interesting in future works.

## 5. ACKNOWLEDGMENT

The authors are grateful to the reviewers for their sound advice.

## 6. CONFLICT OF INTEREST DECLARATION

The authors declare on their honor that this work is not subject to any conflict of interest.

## 7. NOMENCLATURE

| Parameter | Description (unit if defined) | Range of values |
|---|---|---|
| $\wp$ | Set of cells representing the cocoa pod | |
| $a$ | Shape parameter regulating the amplitude of the grooves at the surface of cocoa pod | $\mathbb{R}_+^*$ |
| $b$ | Shape parameter regulating the minimal radius of the cocoa pod | $\mathbb{R}_+^*$ |
| c | Shape parameter regulating the frequency of grooves on the cocoa pod | $\mathbb{R}_+^*$ |
| H | Height of the cocoa pod (*cm*) | $\mathbb{R}_+$ |
| $l$ | Width of the 2D image (pixel) | $\mathbb{N}$ |
| L | Height of the 2D image (pixel) | $\mathbb{N}$ |
| $\varphi$ | Homeomorphism mapping the surface of cocoa pod to a 2D image | |
| $\lambda$ | Invariant unknown parameter governing disease diffusion (*time unit*$^{-1}$) | $\mathbb{R}_+$ |
| $x_i$ | Spatial location of a cell *i* | $\mathbb{R}^3$ |
| $n_{cells}$ | Total number of cells contained in the cocoa pod | $\mathbb{N}$ |
| $\lambda_i$ | Intensity or frequency with which a healthy cell *i* becomes infected (*time unit*$^{-1}$) | $\mathbb{R}_+$ |
| $N_i$ | Set of nearest neighbors of a cell *i* | $\mathbb{N}$ |
| $P_k$ | Set of newly infected cells at the surface of cocoa pod at the *k*-th sampled image | |
| $\lambda_G$ | Global intensity or frequency with which a healthy cells become infected (*time unit*$^{-1}$) | $\mathbb{R}_+$ |
| $\Delta t$ ($t_0$) | Time elapsed between $t_0$ and a new infection (*time*) | $\mathbb{R}_+$ |
| $S_i$ | Boolean variable which is equal to one if cell *i* is healthy | $\{0,1\}$ |
| $d(x_i, x_j)$ | Euclidean distance between the cells $x_i$ and $x_j$ | $\mathbb{R}_+$ |

| | | |
|---|---|---|
| $\omega_{i,k}$ | Apparent intensity with which a healthy cell $i$ at the surface of the cocoa pod becomes infected at the $k$-th sampled image | $\mathbb{R}_+$ |
| $p(t_0, t_0 + dt, i)$ | Probability that a susceptible cell $i$ become infected between times $t_0$ and $t_0 + dt$ | $[0,1]$ |
| $B(p)$ | Bernoulli's distribution with success probability $p$ | $\{0,1\}$ |
| $n = h-1$ | Size of 2D images sample | $\mathbb{N}^*$ |
| $f$ | Marginal conditional probability distribution | $[0,1]$ |
| $L_n$ | Likelihood function base on a sample of size $n$ | $[0,1]$ |
| $N_n$ | Number of infected cells at the surface of cocoa pod | $\mathbb{N}$ |
| $\hat{\lambda}_i$ | Version $i$ of the estimator of $\lambda$ | $\mathbb{R}_+^*$ |
| $AVREE_i$ | Absolute relative error of estimation | $\mathbb{R}_+$ |
| $R^2$ | Determination coefficient of the model | $[0,1]$ |
| $p - value$ | Probability value giving the minimal risk of first species | $[0,1]$ |

## 8. REFERENCES


Abid Hussain, Hongbin Pu, and Da-Wen Sun, 2018. Innovative nondestructive imaging techniques for ripening and maturity of fruits–a review of recent applications. *Trends in Food Science* & *Technology*, **72**, 144–152.

Anuja Bhargava and Atul Bansal, 2018. Fruits and vegetables quality evaluation using computer vision: A review. *Journal of King Saud University-Computer and Information Sciences*.

Bagal M., Belletti G., and Marescotti A., 2013. Etude sur le potentiel de commercialisation du cacao du Cameroun en ''indication géographique''. *Rapport d'étude, Lausanne, REDD, Iram*, page 26.

Barel M., 1985. Technologie du cacao.

Bismark Oduro, Ofosuhene O Apenteng, and Henrietta Nkansah, 2020. Assessing the effect of fungicide treatment on cocoa black pod disease in Ghana: Insight from mathematical modeling. *Statistics, Optimization* & *Information Computing*, **8**(2), 374–385.

Corkidi G., Balderas-Ruız K.A., Taboada B., Serrano-Carreon L. and Galindo E., 2006. Assessing mango anthracnose using a new three-dimensional image-analysis technique to quantify lesions on fruit. *Plant Pathology*, **55**(2), 250–257.

Da Silva C.A., Baker D., Shepherd A.W., Jenaneand C. and Miranda-da-Cruz S., 2009. Agro-industries for development. CABI, FAO and UNIDO, 278p.

Diego Inácio Patrícioa and Rafael Rieder., 2018. Computer vision and artificial intelligence in precision agriculture for grain crops: A systematic review. *Computers and electronics in agriculture*, **153**, 69–81.

Fotsa-Mbogne D.J. and Thron C., 2015. Optimal control of anthracnose using mixed strategies. *Mathematical biosciences*, **269**, 186.

Fotsa-Mbogne D.J., 2018. Estimation of anthracnose dynamics by nonlinear filtering. *International Journal of Biomathematics*, **11**(01), 1850005.

Gardner M., 1970. Mathematical games. *Scientific American*, **222**(6), 132–140.

Gittaly Dhingra, Vinay Kumar, and Hem Dutt Joshi, 2018. Study of digital image processing techniques for leaf disease detection and classification. *Multimedia Tools and Applications*, **77**(15), 19951–20000.

Kanmogne A., Janno Y. and Nganhou J., 2012. Description concise et analyse des systèmes utilisés dans la région sud du Cameroun pour le séchage du cacao. *Tropicultura*, **30**(2), 94–102.

Kleczkowski A., Gilligan C.A. and Bailey D.J., 1997. Scaling and spatial dynamics in plant-pathogen systems: from individuals to populations. *Proceedings of the Royal Society of London. Series B: Biological Sciences*, **264**(1384), 979–984.

Lejeune M., 2004. *Statistique : La théorie et ses applications*. Springer Science & Business Media.

Ling A.S.C., Darmesah G., ChonK.P.g, and Ho C.M., 2019. Application of ARIMAX model to forecast weekly cocoa black pod disease incidence. *Mathematics and Statistics*, **7**(4A), 29–40.

Magrone T., Matteo Antonio Russo, and Emilio Jirillo, 2017. Cocoa and dark chocolate polyphenols: From biology to clinical applications. *Frontiers in Immunology*, **8**, 677.

Marcelo *D*e Carvalho Alves and Edson Ampelio Pozza, 2010. Indicator kriging modeling epidemiology of common bean anthracnose. *Applied Geomatics*, **2**(2), 65–72.

Nader Ekramirad, Akinbode A Adedeji, and Reza Alimardani, 2016. A review of non-destructive methods for detection of insect infestation in fruits and vegetables. Biosystems and Agricultural Engineering Faculty Publications. *Innovations in Food Research*, **2**, 6–12.

Ndoumbe Nkeng M., Efombagn Mousseni I.B., Bidzanga Nomo L., Sache I., and Cilas C., 2017. Spatio-temporal dynamics on a plot scale of cocoa black pod rot caused by phytophthora megakarya in Cameroon. *European Journal of Plant Pathology*, **147**(3), 579–590.

Ndoungue M., Petchayo S., Techou Z., Nana W.G., Nembot C., Fontem D., and Gerben Martijn Ten Hoopen, 2018. The impact of soil treatments on black pod rot (caused by phytophthora megakarya) of cacao in Cameroon. *Biological Control*, **123**, 9–17, 2018.

Nembot C., Takam Soh P., Gerben Martijn Ten Hoopen, and Dumont Y., 2018. Modeling the temporal evolution of cocoa black pod rot disease caused by phytophthora megakarya. *Mathematical Methods in the Applied Sciences*, **41**(18), 8816–8843.

Perrine-Walker F., 2020. Phytophthora palmivora–cocoa interaction. *Journal of Fungi*, **6**(3), 167.

Rady A., Ekramirad N., Adedeji A.A., Li M. and Alimardani R., 2017. Hyperspectral imaging for detection of codling moth infestation in goldrush apples. *Postharvest Biology and Technology*, **129**, 37–44.

Sebastian Anita, Vincenzo Capasso and Simone Scacchi, 2021. Controlling the spatial spread of a xylella epidemic. *Bulletin of Mathematical Biology*, **83**(4), 1–26.

Takoyoh Eyong C., 2003. Poverty eradication and sustainable development in Cameroon. *Journal of Sustainable Development in Africa*, **5**(2), 30–58.

Townsend R.F., Iride Ceccacci, Sanjiva Cook, Mark Constantine, and Moses Gene, 2013. Implementing agriculture for developement: World Bank group agriculture action plan 2013-2015.

Vermolen F. and Polonen I., 2020. Uncertainty quantification on a spatial markov-chain model for the¨ progression of skin cancer. *Journal of Mathematical Biology*, **80**(3), 545–573.

Wood G.A.R. and Lass R.A., 2008. Cocoa, John Wiley & Sons.